

# Jet Precession Driven by Neutrino-Cooled Disc for Gamma-Ray Bursts

Tong Liu<sup>1</sup>, En-Wei Liang<sup>2</sup>, Wei-Min Gu<sup>3</sup>, Xiao-Hong Zhao<sup>1</sup>, Zi-Gao Dai<sup>1</sup>, and Ju-Fu Lu<sup>3</sup>

<sup>1</sup> Department of Astronomy, Nanjing University, Nanjing, Jiangsu 210093, China

<sup>2</sup> Department of Physics, Guangxi University, Nanning, Guangxi, 530004, China

<sup>3</sup> Department of Physics and Institute of Theoretical Physics and Astrophysics, Xiamen University, Xiamen, Fujian 361005, China

Received 2009 / Accepted 2010

## ABSTRACT

**Aims.** A model of jet precession driven by a neutrino-cooled disc around a spinning black hole is present in order to explain the temporal structure and spectral evolution of gamma-ray bursts (GRBs).

**Methods.** The differential rotation of the outer part of a neutrino dominated accretion disc may result in precession of the inner part of the disc and the central black hole, hence drives a precessed jet via neutrino annihilation around the inner part of the disc.

**Results.** Both analytic and numeric results for our model are present. Our calculations show that a black hole-accretion disk system with black hole mass  $M \approx 3.66M_{\odot}$ , accretion rate  $\dot{M} \approx 0.54M_{\odot}s^{-1}$ , spin parameter  $a = 0.9$  and viscosity parameter  $\alpha = 0.01$  may drive a precessed jet with period  $P = 1$  s and luminosity  $L = 10^{51}$  erg  $s^{-1}$ , corresponding to the scenario for long GRBs. A precessed jet with  $P = 0.1$  s and  $L = 10^{50}$  erg  $s^{-1}$  may be powered by a system with  $M \approx 5.59M_{\odot}$ ,  $\dot{M} \approx 0.74M_{\odot}s^{-1}$ ,  $a = 0.1$ , and  $\alpha = 0.01$ , possibly being responsible for the short GRBs. Both the temporal and spectral evolution in GRB pulse may explained with our model.

**Conclusions.** GRB central engines likely power a precessed jet driven by a neutrino-cooled disc. The global GRB lightcurves thus could be modulated by the jet precession during the accretion timescale of the GRB central engine. Both the temporal and spectral evolution in GRB pulse may be due to an viewing effect due to the jet precession.

**Key words.** accretion: accretion discs – black hole physics – gamma rays: bursts

## 1. Introduction

Internal shock models are extensively discussed for gamma-ray bursts (GRBs) (Rees & Mészáros 1992; Mészáros & Rees 1993; Zhang & Mészáros 2004), in which an individual shock episode of two collision shells gives rise to a pulse, and random superposition of pulses results in the observed complexity of GRB light curves (e.g., Daigne & Mochkovitch 1998; Kobayashi et al. 1999). The observed flux rapidly increases in the dynamic timescale of two shell collision, then decays due to the delayed photons from high latitudes with respect to the line of sight upon the abrupt cessation of emission after the crossing timescale, shaping the observed fast-rise-exponential-decay (FRED) pulses. However, some well-separated GRB pulses show symmetric structure, and their peak energy of the  $\nu F_{\nu}$  spectrum ( $E_p$ ) traces the lightcurve behavior (Liang & Kargatis 1996; Liang & Nishimura 2004; Lu & Liang 2009; Peng et al. 2009). Both the temporal and spectral properties of these symmetric pulse are difficult to be explained with internal shocks. In addition, the observed  $E_{\text{iso}} - E_p$  relation (Amati et al. 2002) or  $L_{\text{iso}} - E_p$  relation (Wei & Gao 2003; Liang et al. 2004; Yonetoku et al. 2004) also challenge the internal shock models (e.g., Zhang & Mészáros 2002).

Quasi-periodic feature observed in some GRB light curves motivated ideas that the GRB jet may be precessed (Blackman et al. 1996; Portegies Zwart et al. 1999; Portegies Zwart & Totani 2001; Reynoso et al. 2006; Lei et al. 2007). It is generally believed that the progenitors of short and long GRBs are the mergers of two compact objects (Eichler et al. 1989; Paczyński

1991; Narayan et al. 1992; see recent review by Nakar 2007) and core collapsars of massive stars (Woosley 1993; Paczyński 1998; see reviews by Woosley & Bloom 2006), respectively. Although the progenitors of the two types of GRBs are different, the models for their central engines are similar, and essentially all can be simply classed as a rotating black hole with a rapidly hyper-accreting process of a debris torus surrounding the central black hole. Such a black hole-disk system drives an ultra-relativistic outflow to produce both the prompt gamma-rays and afterglows in lower energy bands. The most popular one is neutrino dominated accretion flows (NDAFs), involving a black hole of  $2 \sim 10M_{\odot}$  and a hyper-critical rate in the range of  $0.01 \sim 10M_{\odot}s^{-1}$  (Popham et al. 1999; Narayan et al. 2001; Kohri & Mineshige 2002; Di Matteo et al. 2002; Kohri et al. 2005, 2007; Lee et al. 2005; Gu et al. 2006; Chen & Beloborodov 2007; Liu et al. 2007, 2008, 2010; Kawanaka & Mineshige 2007; Janiuk et al. 2007). The different direction of angular momentum of two compact objects and the anisotropic fall-back mass in collapsar may conduct precession between black hole and disc. In this scenario, the inner part of the disc is driven by the black hole during the accretion process. The differential rotation between the inner and outer parts may result in precession of the inner part of the disc and the central black hole, hence drive a precessed jet produced by neutrino annihilation around the inner part of the disc, forming an S- or Z-shaped jet as observed in many extragalactic radio sources (see, e.g. Florido et al. 1990). A tilted accretion disc surrounding a black hole would also make the precession of the black hole and result in an S-shaped jet as observed in SS 433 (Sarazin et al. 1980; Lu 1990; Lu & Zhou 2005), although the angle between angular momentum of black hole and disc is small due to that evolution of a two compact

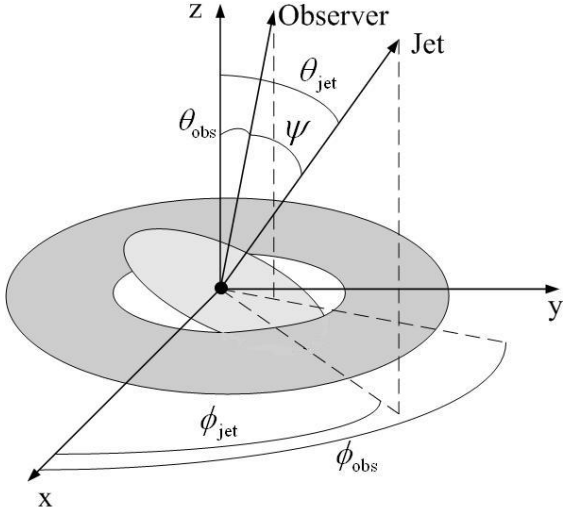


**Fig. 1.** Schematic picture of a precessing system.

object system may decrease the angle between them in mergers or the anisotropic fall-back mass cannot produce large angle between black hole and fall-back mass in collapsars.

In this paper, we propose a model of jet precession driven by a neutrino-cooled disc around a spinning black hole in order to explain the temporal structure and spectral evolution of GRBs. In our model, the global profile of a GRB lightcurve may be modulated by the jet precession. The temporal structure and spectral evolution may signal an on-axis/off-axis cycle of the light of sight (LOS) to a precessed jet axis, as proposed by some authors to explain the nature of low luminosity GRBs 980425 and 031203 (Nakamura 1998; Eichler & Levinson 1999; Waxman 2004; Ramirez-Ruiz et al. 2005) or to present a unified model for GRBs and X-ray flashes (Yamazaki et al. 2003) and the observed spectral lag in long GRBs (Norris 2002; Salmonson & Galama 2002).

We present both analytic and numerical analysis for jet precession driven by a neutrino-cooled disc around a spinning black hole in sections 2 and 3. Simplifying the jet emission surface as a point source, we demonstrate the profile and evolution of a GRB pulse in section 4. Conclusions and discussion are shown in section 5.

## 2. Model

An accretion disk would be warped by its precession (Sarazin et al. 1980). We consider a spinning black hole surrounding a tilted accretion disc that its rotation axis is misaligned with that of the black hole, as shown in Fig. 1. Its angular momentum is  $J_* = aGM^2/c$ , where  $M$  is the black hole mass and  $a$  ( $0 < a < 1$ ) is the dimensionless specific angular momentum. Since  $dJ = 2\pi r^2 \Sigma v_\phi dr$  for a ring at radius  $r$  in the disc with width  $dr$ , we get  $J(r) = dJ/d(\ln r) = 2\pi r^3 \Sigma v_\phi$ , where  $\Sigma$  and  $v_\phi$  are the disk surface density and rotational velocity. Due to the Lense-Thirring effect (Lense & Thirring 1918), the disc material interior to a critical radius  $r_p$ , which is defined as  $J(r_p) = J_*$ , will be aligned with the equatorial plane of the black hole. The outer portion of the disc ( $r \gtrsim r_p$ ) with sufficiently large angular momentum keeps its orientation. This makes the black hole precess along with the inner disc (Bardeen & Petterson 1975). A jet dominated by the ejections of neutrino annihilation around the inner part of the disc thus would be precessed (Popham et al. 1999; Liu et al.

2007). The precession rate  $\Omega$  of the central black hole and the inner disc is given by  $\Omega = 2GJ(r)/c^2 r^3$  (Sarazin et al. 1980). Note that regions with  $r \gtrsim r_p$  in the disc should contribute to the precession. The  $\Omega$  decreases as  $r$  increases, so one cannot expect a period behavior in an observed light curve from our model.

With the continuity equation

$$\dot{M} = -2\pi r \Sigma v_r, \quad (1)$$

the precession period  $P$  then can be expressed as

$$P \equiv \frac{2\pi}{\Omega} = (\pi M) \left( \frac{a}{G} \right)^{\frac{1}{2}} \left( \frac{c v_r}{\dot{M} v_\phi} \right)^{\frac{3}{2}}, \quad (2)$$

where  $\dot{M}$  is the accretion rate and  $v_r$  the radial inflow velocity of the disc material. Assuming that the angular velocity is approximately Keplerian, we have  $v_\phi = r\Omega_K$ , and the vertical scale height of the flow can be written as  $H = c_s/\Omega_K$ , where  $\Omega_K = (GM/r^3)^{1/2}$  and  $c_s$  are the Keplerian angular velocity and the sound speed, respectively. The  $v_r$  can be estimated as  $v_r \sim \alpha c_s (H/r)$  (Kato et al. 2008), where  $\alpha$  is the constant viscosity parameter of the disc. Substituting the expressions of  $v_\phi$  and  $v_r$  into equation (3), we have

$$P = 1.42 \times 10^3 a^{\frac{1}{2}} \alpha^{\frac{3}{2}} \left( \frac{M}{M_\odot} \right) \left( \frac{\dot{M}}{M_\odot s^{-1}} \right)^{-\frac{3}{2}} \left( \frac{H}{r} \right)^3 s. \quad (3)$$

It is found that  $P$  is sensitive to  $\alpha$ ,  $\dot{M}$  and  $H/r$ . These parameters are time-dependent in the GRB phenomenon; hence the precession period should evolve with time. Regions with  $r \gtrsim r_p$  in the disc should contribute to the precession, and the evolution of the hyper-accretion process would make the mass and the angular momentum of black hole increase (Belczyński et al. 2008; Janiuk et al. 2008), hence make evolution of the precession period. In addition, the nutation in the accretion system even makes the observed profile be much complicated. Therefore, one cannot expect clear period information in the GRB lightcurves. If the periods are shorter than the accretion timescale, the observed lightcurve may be composed of some pulses. Occasionally, the lightcurves may show quasi-periodic feature, such as that observed in BATSE trigger 1425 (Portegies Zwart et al. 1999). If the periods are longer than the accretion timescale, the global lightcurve may be a broad pulse. This is different from that for SS433 (Sarazin et al. 1983), in which it is assumed that the precession periods are shorter than the viscous timescale without rapidly evolving with time, hence the periodic lightcurve is a natural consequence in SS 433.

## 3. Numerical Results

The Eq. (3) show an explicit dependence of  $P$  to  $a$ ,  $\alpha$ ,  $\dot{M}$ ,  $M$ , and  $H/r$ . However, the thickness of NDAF also depends on  $M$ ,  $\dot{M}$ ,  $a$  and  $\alpha$ . Similar to  $P$ , the injected neutrino annihilation luminosity  $L$  is also a function of these parameters. In order to illustrate both the dependences of  $P$  and  $L$  on these parameters, we present numerical calculation with the method by Riffert & Herold (1995). This method defines general relativistic correction factors to simulate the precession period related to the spin of a black hole. They are written as

$$A = 1 - \frac{2GM}{c^2 r} + \left( \frac{aGM}{c^2 r} \right)^2, \quad (4)$$

$$B = 1 - \frac{3GM}{c^2 r} + 2a \left( \frac{aGM}{c^2 r} \right)^{\frac{3}{2}}, \quad (5)$$

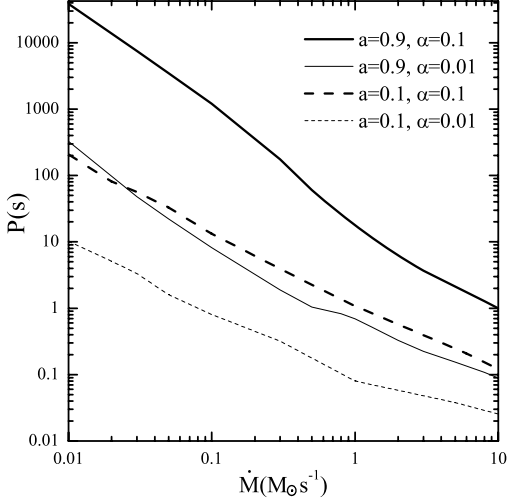


**Fig. 2.** Illustration of numerical results for  $P$  as a function of  $\dot{M}$  using different parameter sets as marked in the plot.

$$C = 1 - 4a \left( \frac{aGM}{c^2 r} \right)^{\frac{3}{2}} + 3 \left( \frac{aGM}{c^2 r} \right)^2 \quad (6)$$

$$D = \int_{r_{ms}}^r \frac{\frac{x^2 c^4}{2G^2} - \frac{3xMc^2}{G} + 4 \left( \frac{xa^2 M^3 c^2}{G} \right)^{\frac{1}{2}} - \frac{3a^2 M^2}{2}}{(xr)^{\frac{1}{2}} \left[ \frac{x^2 c^4}{G^2} - \frac{3xMc^2}{G} + 2 \left( \frac{xa^2 M^3 c^2}{G} \right)^{\frac{1}{2}} \right]} dx, \quad (7)$$

where  $r_{ms}$  is the inner boundary of the disc. The equation of conservation of mass remains valid, while hydrostatic equilibrium in the vertical direction leads to a corrected expression for the half thickness of the disc (Riffert & Herold 1995),

$$H \simeq c_s \left( \frac{r^3}{GM} \right)^{\frac{1}{2}} \left( \frac{B}{C} \right)^{\frac{1}{2}}, \quad (8)$$

where  $c_s = (p/\rho)^{1/2}$ ,  $p$  and  $\rho$  are the total pressure and density of the disc, respectively. The viscous shear  $T_{r\phi}$  is also corrected as

$$T_{r\phi} = -\alpha p \left( \frac{A}{BC} \right)^{\frac{1}{2}}, \quad (9)$$

and the angular momentum equation can be simplified as (Riffert & Herold 1995, Lei et al. 2009)

$$T_{r\phi} = \frac{\dot{M}}{4\pi H} \left( \frac{GM}{r^3} \right)^{\frac{1}{2}} \left( \frac{D}{A} \right)^{\frac{1}{2}}. \quad (10)$$

The equation of state is

$$p = p_{\text{gas}} + p_{\text{rad}} + p_e + p_\nu, \quad (11)$$

where  $p_{\text{gas}}$ ,  $p_{\text{rad}}$ ,  $p_e$ , and  $p_\nu$  are the gas pressure from nucleons, radiation pressure of photons, degeneracy pressure of electrons, and radiation pressure of neutrinos, respectively (see, e.g. Di Matteo et al. 2002; Liu et al. 2007). The energy equation is written as

$$Q_{\text{vis}} = Q_{\text{adv}} + Q_{\text{photo}} + Q_\nu, \quad (12)$$

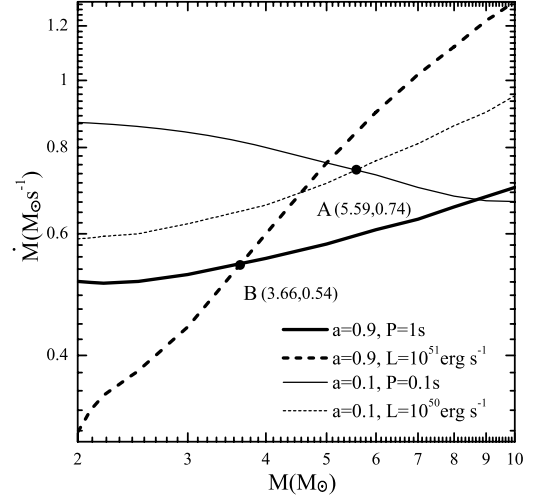


**Fig. 3.**  $\dot{M}$  as a function of  $M$  for different parameter sets as marked in the plot. The viscosity parameter is adopted as  $\alpha = 0.01$ . The Two interaction points A and B indicate estimates of  $M$  and  $\dot{M}$  for a given set of  $(P, L, a, \alpha)$ .

where  $Q_{\text{vis}}$ ,  $Q_{\text{adv}}$ ,  $Q_{\text{photo}}$  and  $Q_\nu$  are the viscous heating rate, the advective cooling rate, the cooling rate due to photodisintegration of  $\alpha$ -particles and the cooling due to the neutrino radiation, respectively (see, e.g. Di Matteo et al. 2002; Liu et al. 2007). The heating rate  $Q_{\text{vis}}$  is expressed as

$$Q_{\text{vis}} = \frac{3GM\dot{M}D}{8\pi r^3 B}. \quad (13)$$

The equation system consisting of Eqs. (1), (2), (4)-(13) is closed for an unknown precession period  $P$ . It can be numerically solved for a given parameter set of  $M$ ,  $\dot{M}$ ,  $a$ , and  $\alpha$ . We show  $P$  as a function of  $\dot{M}$  for the parameter sets ( $a = 0.9$ ,  $M = 3M_\odot$ ,  $\alpha = 0.01$ ), ( $a = 0.9$ ,  $M = 3M_\odot$ ,  $\alpha = 0.1$ ), ( $a = 0.1$ ,  $M = 3M_\odot$ ,  $\alpha = 0.1$ ) and ( $a = 0.1$ ,  $M = 3M_\odot$ ,  $\alpha = 0.01$ ) in Fig. 2. It is found that  $P$  varies from tens of milliseconds to 10 ks, if  $\dot{M} = 0.01 \sim 10 M_\odot/\text{s}$ ,  $\alpha = 0.01 \sim 0.1$ , and  $a = 0.1 \sim 0.9$ . It can approach the timescale of lightcurve or be longer than the accretion timescale whose provide a couple of possibilities of lightcurve. In collapsar scenario, the central black hole would be rapidly rotates, i.e.,  $a \gtrsim 0.9$ . For the compact object mergers, the spin of the black hole is not strictly as high as that in the collapsar scenario (e.g., van Putten et al. 2001). Assuming that the global GRB lightcurves are modulated by the jet precession during the accretion timescale of the GRB central engine, the profile of a pulse duration may be comparable to  $P$ . Statistical analysis shows that the typical durations of long and short GRB pulses are  $\sim 1$  and  $0.1$  second, respectively (Liang et al. 2002; Nakar & Piran 2002). From Fig. 2, we find that the case of ( $\alpha = 0.1$ ,  $a = 0.9$ ) yields a  $P$  value much larger than 1 seconds in the range of  $\dot{M} = 0.01 \sim 10 M_\odot$ . For the case of ( $\alpha = 0.01$ ,  $a = 0.9$ ), we get  $P = 0.1 \sim 1$  seconds for  $\dot{M} = 0.4 \sim 10 M_\odot$ . This is consistent with the observed pulse durations for long GRBs. In order to explain the duration of short GRB pulses, our model requires lower  $a$  and  $\alpha$  as well as higher  $\dot{M}$  than that for the long GRBs, indicating that the short duration GRBs may be powered by much violent accretion process than the long ones.

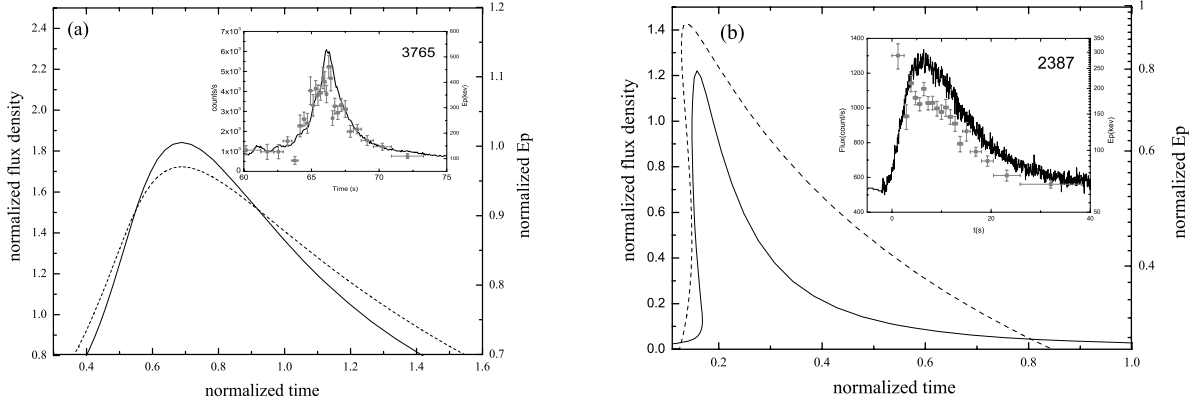


**Fig. 4.** Predicted flux  $F$  (the solid line) and  $E_p$  (the dashed line) with our model for a symmetric pulse (panel a) and a FRED pulse (panel b) with comparisons to the observations (insets).

The observed luminosity of prompt gamma-rays may also place constraints on our model parameters. We assume that the observed gamma-ray luminosity is comparable to the injected neutrino annihilation luminosity  $L$ . Similar to  $P = P(M, \dot{M}, a, \alpha)$ ,  $L$  is a function of  $M$ ,  $\dot{M}$ ,  $a$ , and  $\alpha$ , written as  $L = L(M, \dot{M}, a, \alpha)$ . It can be calculated following the approach of Ruffert et al (1997), Popham et al (1999), Rosswog et al (2003), and Liu et al (2007). Since the calculation of  $L$  (or  $P$ ) as a function of these parameters is a huge time-consuming task, we perform our calculation for typical  $L$  values only and present our results with  $\dot{M}$  as a function of  $M$ ,  $a$ ,  $\alpha$  for a given  $L$  (or  $P$ ). We take  $L = 10^{51} \text{ erg s}^{-1}$  for long GRBs and  $L = 10^{50} \text{ erg s}^{-1}$  for short GRBs. Based on our analysis above, we also calculate  $\dot{M}$  as a function of  $M$  for  $P = 1 \text{ s}$  and  $P = 0.1 \text{ s}$  in case of parameter set  $(L, a, \alpha) = (10^{51} \text{ erg s}^{-1}, 0.9, 0.01)$  and  $(L, a, \alpha) = (10^{50} \text{ erg s}^{-1}, 0.1, 0.01)$ . We show  $\dot{M}$  as a function of  $M$  for different parameter sets in Fig. 3. It is found that for a given luminosity,  $\dot{M}$  as a function of  $M$  greatly depends on the rotation of the black hole (see the dotted lines in Fig. 3). The accretion rate  $\dot{M}$  does not significantly increase with  $M$  for  $a = 0.1$ . However, it rapidly increases with  $M$  for  $a = 0.9$ . The behavior of the function  $\dot{M}(M)$  varies for different  $P$  (see the solid lines in Fig. 3). As shown in Fig. 3,  $\dot{M}$  slightly increases with  $M$  if  $P = 1 \text{ second}$ . However, it even decreases with  $M$  for  $P = 0.1 \text{ second}$ . This conflicts with that shown in the explicit form of  $P$  (see Eq. 3). The reason is that the thickness of NDAF depends on  $M$ ,  $\dot{M}$ ,  $a$  and  $\alpha$  (see Fig. 9 in Liu et al. 2007). One cannot expect an explicit dependence between  $\dot{M}$  and  $M$  for a given  $P$ . The intersections between the lines are estimates of  $M$  and  $\dot{M}$  for a given set of  $(P, L, a, \alpha)$ . We find that  $M \approx 3.66 M_\odot$  and  $\dot{M} \approx 0.54 M_\odot \text{ s}^{-1}$  for  $P = 1 \text{ s}$ ,  $L = 10^{51} \text{ erg s}^{-1}$ , and  $a = 0.9$ , corresponding to the scenario for long GRBs. For  $P = 0.1 \text{ s}$ ,  $L = 10^{50} \text{ erg s}^{-1}$ , and  $a = 0.1$ , we get  $M \approx 5.59 M_\odot$  and  $\dot{M} \approx 0.74 M_\odot \text{ s}^{-1}$ , corresponding to the scenario for short GRBs. These solutions are generally consistent with the requirements of GRB productions in simulations for collapsars (e.g. MacFadyen & Woosley 1999) and for binary coalescence of a neutron star and a black hole or two neutron stars (e.g. Kluźniak & Lee 1998).

#### 4. Temporal Profile and Spectral Evolution of a GRB Pulse from a Precessing Jet

As discussed above, in the framework of our model one cannot expect period information from the observed lightcurves since the precession period is time-dependent. Since the period is a function of some time-dependent parameters as mentioned above, temporal profile and spectral evolution of pulses in GRB lightcurves may be a direct information of jet precession since the jet precession may conduct an on-axis/off-axis cycle during a precession period for a given observer.

As discussed in Section 1, the  $E_p$ -tracing-flux spectral evolution feature is observed in some GRB pulses (e.g. Liang et al. 1996; Peng et al. 2009; Lu & Liang 2009). The profiles of these pulses are generally FRED, and occasionally are symmetrical. These temporal and spectral features can be explained with our model. We just illustrate the lightcurve and the spectral evolution for a point source with arbitrary radiation intensity in the axis with an arbitrary precession period with ultra-relativistic velocity in the jet axis. As shown by Granot et al. (2002), assuming the emitting region as a point source in the jet axis, the calculation can give reasonable results without any assumption on the jet structure. Therefore, we adopt the point source assumption in our calculations. We just illustrate the lightcurve and the spectral evolution for a point source with arbitrary radiation intensity in the axis with an arbitrary precession period for an observer (on-axis and off-axis) at the rest frame in Section 4. If the emitting region is a shell of the jet with certain opening angle, the peak of the pulse would be flattened in case of a uniform jet. Our calculation is followed by that present in Granot et al. 2002.

The observed flux  $F$  and  $E_p$  would be amplified due to the Doppler effect,  $F = F_0(1-\beta)^3/(1-\beta\cos\Psi)^3$ ,  $E_p = E_{p0}(1-\beta)/(1-\beta\cos\Psi)$ . The observed time scale would be  $t = t_0(1-\beta\cos\Psi)/(1-\beta)$ , where the subscript 0 means the “on-axis” quantities,  $\Psi$  is the view angle between the jet axis and the LOS and  $\beta = (\Gamma^2 - 1)^{1/2}/\Gamma$ ,  $\Gamma$  is the Lorentz factor. From Fig. 1, we have

$$\cos\Psi = \cos\theta_{\text{jet}}\cos\theta_{\text{obs}} + \sin\theta_{\text{jet}}\sin\theta_{\text{obs}}\cos(\phi_{\text{jet}} - \phi_{\text{obs}}), \quad (14)$$

where  $\phi_{\text{jet}} = \phi_{\text{jet},0} + 2\pi t_1/P$  ( $t_1$  is the time in the rest frame of the central engine) and  $z$ -axis in Fig. 1 is the direction of angular

momentum of the outer part. We assume  $\Gamma = 300$  in our calculations. We compute the observed flux and peak energy of the  $\nu F_\nu$  spectrum in a precession period corresponding to an observed pulse. Figure 4 demonstrates the initial “off-axis” and initial “on-axis” lightcurves and corresponding  $E_p$  evolutions for an point source with arbitrary flux intensity and spectral hardness in the jet with arbitrary precession period  $P$ . The adopted parameters are  $\theta_{\text{obs}} = 1^\circ$ ,  $\phi_{\text{obs}} = 90^\circ$ ,  $\theta_{\text{jet}} = 4^\circ$ , and  $\phi_{\text{jet},0} = 0^\circ$  for initial “off-axis” observer and  $\theta_{\text{obs}} = 1^\circ$ ,  $\phi_{\text{obs}} = 90^\circ$ ,  $\theta_{\text{jet}} = 2^\circ$  and  $\phi_{\text{jet},0} = 0^\circ$  for initial “on-axis” observers. Two samples of the observations are also shown in Fig. 4 for comparisons. It is found that our model can re-produce both FRED and symmetric pulses with  $E_p$ -tracing-flux behavior, depending on the initial on-axis of off-axis observations.

## 5. Conclusions

We have suggested that the differential rotation of the outer part of a neutrino dominated accretion disc may result in precession of the central black hole and the inner part of the disc, hence may power a precessed jet via neutrino annihilation around the inner part of the disc. Both analytic and numeric results are present. Our calculations show that for a black hole-accretion disk system with  $M \simeq 3.66M_\odot$ ,  $\dot{M} \simeq 0.54M_\odot\text{s}^{-1}$ ,  $a = 0.9$  and  $\alpha = 0.01$  may drives a precessed jet with  $P = 1$  s and  $L = 10^{51}$  erg  $\text{s}^{-1}$ , corresponding to the scenario for long GRBs. A precessed jet with  $P = 0.1$  s and  $L = 10^{50}$  erg  $\text{s}^{-1}$  may be powered by a system with  $M \simeq 5.59M_\odot$ ,  $\dot{M} \simeq 0.74M_\odot\text{s}^{-1}$ ,  $a = 0.1$ , and  $\alpha = 0.01$ , possibly being responsible for the short GRBs. These results are generally consistent with simulations for long and short GRB productions from collapsars and from mergers of compact stars. Both temporal and spectral features observed in GRB pulses may be explained with our model.

The correlation between  $E_{\text{iso}}$  (or  $L_{\text{iso}}$ ) and  $E_p$  in the burst frame (Amati et al. 2002; Liang et al. 2004) are difficult to be explained in the framework of internal shock scenarios. Our model suggests an  $E_p$ -tracing-flux behavior within a GRB pulse due to the on-axis/off-axis effect for a given observer, similar to that proposed by Yamazaki et al. (2004). The  $E_p$ -tracing-flux behavior would give rise to the observed correlations between  $E_{\text{iso}}$  ( $L_{\text{iso}}$ ) and  $E_p$  in the burst frame.

## acknowledgments

We thank the anonymous referee for very useful comments. We also thank Bing Zhang, Shuang-Nan Zhang, Li-Xin Li, and Wei-Hua Lei for beneficial discussion. This work was supported by the China Postdoctoral Science Foundation funded project 20080441038 (T.L.), the National Natural Science Foundation of China under grants 10778711 (W.M.G.), 10833002 (J.F.L. and W.M.G.), 10873002 (E.W.L.), 10873009 (Z.G.D.), the National Basic Research Program (973 Program) of China under Grant 2009CB824800 (E.W.L., W.M.G., and J.F.L.). E. W. L. also acknowledges the support from Guangxi SHI-BAI-QIAN project (Grant 2007201), the program for 100 Young and Middle-aged Disciplinary Leaders in Guangxi Higher Education Institutions, and the research foundation of Guangxi University(M30520).

## References

Amati, L., et al. 2002, A&A, 390, 81  
 Bardeen, J. M., & Petterson, J. A. 1975, ApJ, 195, L65  
 Belczyński, K., Taam, R. E., Rantsiou, E., & van der Sluys, M. 2008, ApJ, 682, 474

Blackman, E. G., Yi, I., & Field, G. B. 1996, ApJ, 473, L79  
 Chen, W.-X., & Beloborodov, A. M. 2007, ApJ, 657, 383  
 Daigne, F., & Mochkovitch, R. 1998, MNRAS, 296, 275  
 Di Matteo, T., Perna, R., & Narayan, R. 2002, ApJ, 579, 706  
 Eichler, D., & Levinson, A. 1999, ApJ, 521, L117  
 Eichler, D., Livio, M., Piran, T., & Schramm, D. N. 1989, Nature, 340, 126  
 Florido, E., Battaner, E., & Sanchez-Saavedra, M. L. 1990, Ap&SS, 164, 131  
 Granot, J., Panaitescu, A., Kumar, P., & Woosley, S. E. 2002, ApJ, 570, 61  
 Gu, W.-M., Liu, T., & Lu, J.-F. 2006, ApJ, 643, L87  
 Janiuk, A., Moderski, R., & Proga, D. 2008, ApJ, 687, 433  
 Janiuk, A., Yuan, Y.-F., Perna, R., & Di Matteo, T. 2007, ApJ, 664, 1011  
 Kato, S., Fukue, J., & Mineshige, S. 2008, Black-Hole Accretion Discs (Kyoto: Kyoto Univ. Press)  
 Kawanaka, N., & Mineshige, S. 2007, ApJ, 662, 1156  
 Kluźniak, W., & Lee, W. H. 1998, ApJ, 494, L53  
 Kobayashi, S., Piran, T., & Sari, R. 1999, ApJ, 513, 669  
 Kohri, K., & Mineshige, S. 2002, ApJ, 577, 311  
 Kohri, K., Narayan, R., & Piran, T. 2005, ApJ, 629, 341  
 Kohri, K., Ohsuga, K., & Narayan, R. 2007, MNRAS, 381, 1267  
 Lee, W. H., Ramirez-Ruiz, E., & Page, D. 2005, ApJ, 632, 421  
 Lei, W. H., Wang, D. X., Gong, B. P., & Huang, C. Y. 2007, A&A, 468, 563L  
 Lei, W. H., Wang, D. X., Zhang, L., Gan, Z. M., Zou, Y. C., & Xie, Y. 2009, ApJ, 700, 1970  
 Lense, J., & Thirring, H. 1918, Phys. Z., 19, 156  
 Liang, E., & Kargatis, V. 1996, Nature, 381, 49  
 Liang, E., & Nishimura, K. 2004, Physical Review Letters, 92, 175005  
 Liang, E.-W., Dai, Z.-G., & Wu, X.-F. 2004, ApJ, 606, L29  
 Liang, E.-W., Xie, G.-Z., & Su, C.-Y. 2002, PASJ, 54, 1  
 Liu, T., Gu, W.-M., Dai, Z.-G., & Lu, J.-F. 2010, ApJ, 709, 851  
 Liu, T., Gu, W.-M., Xue, L., & Lu J.-F. 2007, ApJ, 661, 1025  
 Liu, T., Gu, W.-M., Xue, L., Weng, S.-S., & Lu J.-F. 2008, ApJ, 676, 545  
 Lu J.-F. 1990, A&A, 229, L424  
 Lu J.-F., & Zhou, B.-Y. 2005, ApJ, 635, L17  
 Lu R.-J. & Liang E.-W., Science in China, 2009, submitted  
 MacFadyen, A. I., & Woosley, S. E. 1999, ApJ, 524, 262  
 Mészáros, P., & Rees, M. J. 1993, ApJ, 405, 278  
 Nakamura, T. 1998, Prog. Theor. Phys., 100, 921  
 Nakar, E., & Piran, T. 2002, MNRAS, 331, 40  
 Nakar, E. 2007, Phys. Rep., 442, 166  
 Narayan, R., Paczynski, B., & Piran, T. 1992, ApJ, 395, L83  
 Narayan, R., Piran, T., & Kumar, P. 2001, ApJ, 557, 949  
 Norris, J. P. 2002, ApJ, 579, 386  
 Paczyński, B. 1991, Acta Astron., 41, 257  
 Paczyński, B. 1998, ApJ, 494, L45  
 Peng, Z.-Y., Ma, L., Zhao, X.-H., Yin, Y., Fang, L.-M., & Bao, Y.-Y. 2009, ApJ, 698, 417  
 Popham, R., Woosley, S. E., & Fryer, C. 1999, ApJ, 518, 356  
 Portegies Zwart, S. F., Lee, C. H., & Lee, H. K. 1999, ApJ, 529, 666  
 Portegies Zwart, S. F., & Totani, T. 2001, ApJ, 328, 951  
 Ramirez-Ruiz, E., Granot, J., Kouveliotou, C., Woosley, S. E., Patel, S. K., & Mazzali, P. A. 2005, ApJ, 625, L91  
 Rees, M. J., & Mészáros, P. 1992, MNRAS, 258, 41  
 Reynoso, M. M., Romero, G. E., & Sampayo, O. A. 2006, A&A, 454, 11  
 Riffert, H., & Herold, H. 1995, ApJ, 450, 508  
 Rosswog, S., Ramirez-Ruiz, E., & Davies, M. B. 2003, MNRAS, 345, 1077  
 Ruffert, M., Janka, H.-Th., Takahashi, K., & Schäfer, G. 1997, A&A, 319, 122  
 Salmonson, J. D., & Galama, T. J. 2002, ApJ, 569, 682  
 Sarazin, C. L., Begelman, M. C., & Hatchett, S. P. 1980, ApJ, 238, L129  
 van Putten, M. H. P. M., & Ostriker, E. C. 2001, ApJ, 552, L31  
 Waxman, E. 2004, ApJ, 602, 886  
 Wei, D. M., & Gao, W. H. 2003, MNRAS, 345, 743  
 Woosley, S. E. 1993, ApJ, 405, 273  
 Woosley, S. E., & Bloom, J. S. 2006, ARA&A, 44, 507  
 Yamazaki, R., Ioka, K., & Nakamura, T. 2004, ApJ, 606, L33  
 Yamazaki, R., Yonetoku, D., & Nakamura, T. 2003, ApJ, 594, L79  
 Yonetoku, D., Murakami, T., Nakamura, T., Yamazaki, R., Inoue, A. K., & Ioka, K. 2004, ApJ, 609, 935  
 Zhang, B., & Mészáros, P. 2002, ApJ, 581, 1236  
 Zhang, B., & Mészáros, P. 2004, Int. J. Mod. Phys. A, 19, 2385